Published in final edited form as:
Mol Cancer Ther. 2008 October ; 7(10): 3256–3264. doi:10.1158/1535-7163.MCT-08-0157.

Cisplatin Abrogates the Geldanamycin-induced Heat Shock Response

Andrea K. McCollum[1], **Kara B. Lukasiewicz**[2,3], **Cynthia J. TenEyck**[5], **Wilma L. Lingle**[2,3,4], **David O. Toft**[3], and **Charles Erlichman**[5]

1 *Department of Molecular Pharmacology and Experimental Therapeutics, Mayo Clinic College of Medicine, Rochester, Minnesota*

2 *Tumor Biology Program, Mayo Clinic College of Medicine, Rochester, Minnesota*

3 *Department of Biochemistry and Molecular Biology, Mayo Clinic College of Medicine, Rochester, Minnesota*

4 *Department of Experimental Pathology, Mayo Clinic College of Medicine, Rochester, Minnesota*

5 *Department of Oncology, Mayo Clinic College of Medicine, Rochester, Minnesota*

Abstract

Benzoquinone ansamycin antibiotics such as geldanamycin (GA) bind to the N-terminal ATP binding domain of Hsp90 and inhibit its chaperone functions. Despite *in vitro* and *in vivo* studies indicating promising antitumor activity, derivatives of GA, including 17-AAG have demonstrated little clinical efficacy as single agents. Thus, combination studies of 17-AAG and several cancer chemotherapeutics, including cisplatin (CDDP), have begun. In colony-forming assays, the combination of CDDP and GA or 17-AAG was synergistic, and caused increased apoptosis compared to each agent alone. One measurable response that results from treatment with Hsp90-targeted agents is the induction of an HSF-1 heat shock response. Treatment with GA + CDDP revealed that CDDP suppresses upregulation of HSF-1 transcription, causing decreased levels of stress-inducible proteins such as Hsp27 and Hsp70. However, CDDP treatment did not prevent trimerization and nuclear localization of HSF-1, but inhibited DNA binding of HSF-1 as demonstrated by chromatin immunoprecipitation. Melphalan, but not camptothecin, caused similar inhibition of GA-induced HSF-1-mediated Hsp70 upregulation. MTS cell survival assays revealed that deletion of Hsp70 caused increased sensitivity to GA ($Hsp70^{+/+}$ IC_{50}=63.7±14.9 nM and $Hsp70^{-/-}$ IC_{50}=4.3±2.9 nM), which confirmed that a stress response plays a critical role in decreasing GA sensitivity. Our results suggest that the synergy of GA + CDDP is due, in part, to CDDP-mediated abrogation of the heat shock response through inhibition of HSF-1 activity. Clinical modulation of the HSF-1-mediated heat shock response may enhance the efficacy of Hsp90-directed therapy.

Keywords

17-AAG; Geldanamycin; Cisplatin; Hsp90; HSF-1

Reprint Requests: Charles Erlichman, Department of Oncology, Guggenheim 1311A, Mayo Clinic, 200 1st Street SW, Rochester, MN 55905, Tel. 507 284-3514; Fax. (507) 266-5146; E-mail: erlichman.charles@mayo.edu.

Conflict of Interest Statement: C. Erlichman was co-investigator for a 17-AAG clinical trial funded by Conforma Therapeutics. The other authors have no potential conflicts of interest to disclose.

Introduction

Hsp90 is a molecular chaperone that contributes to cellular homeostasis by participating in several processes, including folding nascent proteins, stabilizing unfolded proteins to prevent aggregation, and facilitating intracellular trafficking. ATP hydrolysis is critical for Hsp90 chaperone functions, driving clamp-like reactions to facilitate protein folding (1). Benzoquinone ansamycins such as GA and its derivative 17-AAG bind to the N-terminal ATP binding domain of Hsp90 and lock it into an ADP-bound conformation (2–6). At least two measurable cellular responses ensue. First, proteins that rely on Hsp90 are degraded by the proteasome after treatment with GA. These proteins, referred to as clients, are normally stabilized and folded into a functional state by the Hsp90 chaperone complex. However, GA binding disrupts the interaction of these proteins with the Hsp90 chaperone complex, preventing normal folding and leading to ubiquitylation and subsequent degradation (7–9). Second, GA treatment induces upregulation of many proteins through the action of the transcription factor heat shock factor-1 (HSF-1) (10–13). These newly synthesized proteins then work to restore cellular homeostasis after disruption of Hsp90 function.

17-AAG is currently in Phase 2 clinical trials as a single agent, and Phase 1 trials in combination with other cancer therapeutics. Despite promising preclinical studies demonstrating significant anti-tumor activity *in vitro* and *in vivo* (14–16), 17-AAG has produced little clinical impact thus far as a single agent (8,17). This lack of activity has prompted studies to determine possible resistance mechanisms to 17-AAG. While tumor cell sensitivity to 17-AAG might be mediated, at least in part, by the presence of overexpressed client proteins such as Her-2 (18,19), recent studies have indicated that the upregulation of stress-responsive proteins, particularly Hsp70 and Hsp27, after Hsp90 inhibition, might also be responsible for the poor activity observed in 17-AAG clinical trials (10,12,20). Interest in these stress response proteins as a factor in resistance to Hsp90-directed therapy has been supported by data from several studies. Not only has Hsp70 been shown to inhibit changes in conformation and localization of Bax, thereby preventing apoptosis, but downregulation of Hsp70 also sensitizes tumor cells to 17-AAG (21,22). Moreover, Hsp27 upregulation has been shown to contribute to 17-AAG resistance through a glutathione-mediated mechanism (23). Additionally, KNK437, a benzylidene lactam compound that suppresses the cellular heat shock response, has been shown to sensitize cells to Hsp90-directed agents (21).

Taken together these studies indicate that circumventing HSF-1-mediated upregulation of stress-responsive proteins provides an opportunity to increase the efficacy of Hsp90-directed therapy. After treatment with GA, HSF-1 is released from a Hsp90-containing heterocomplex that normally serves to repress HSF-1 transcriptional activity (24–26). HSF-1 then collects in the nucleus within large and brightly staining nuclear stress granules to eventually drive transcription of stress-responsive genes (27,28). After trimerization and post-translational modifications such as phosphorylation, HSF-1 binds to highly conserved promoter sequences called heat shock elements (HSEs) (29,30) and stimulates transcription of stress-inducible proteins, including Hsp70 and Hsp27, up to 1000-fold compared to unstressed conditions (31). Each of these activation steps for HSF-1 offers a prospect for pharmacological intervention that could enhance efficacy of Hsp90-directed agents by limiting Hsp70 and Hsp27 upregulation.

In this study, we demonstrate that combining cisplatin (CDDP) with GA or 17-AAG results in synergistic tumor cell killing. To define a mechanism for this synergy, we have investigated the contribution of HSF-1-mediated heat shock response upregulation. Our data indicate that CDDP blocks GA-induced HSF-1-mediated transcription, resulting in decreased stress-responsive protein levels after treatment. The decreased transcription observed when GA is combined with CDDP is due to CDDP-mediated abrogation of HSF-1 chromatin binding,

thereby preventing upregulation of stress-responsive transcripts for genes such as Hsp70 and Hsp27. We have also identified melphalan (MEL) as another agent that enhances 17-AAG efficacy by blocking the upregulation of stress-responsive proteins. Taken together, our data demonstrate that chemotherapeutics such as CDDP and MEL may be useful for preventing 17-AAG resistance by blocking the upregulation of stress-responsive proteins such as Hsp70 and Hsp27.

Materials and Methods

Materials

Reagents were obtained from the following sources: GA and 17-AAG from Dr. V.L. Narayanan, Drug Synthesis and Chemistry Branch, National Cancer Institute (Bethesda, MD); CDDP, MEL, and camptothecin (CPT) from Sigma (St Louis, MO); and ECL enhanced chemiluminescent reagents from Amersham Pharmacia Biotechnology (Piscataway, NJ).

Antibodies

H9010 mouse monoclonal antibody recognizing Hsp90 was previously described (32). The remaining antibodies were purchased from the following suppliers: peroxidase-coupled affinity-purified goat anti-mouse and goat anti-rabbit secondary antibodies from Kirkegaard & Perry (Gaithersburg, MD); mouse monoclonal anti-Hsp70, rabbit polyclonal HSF-1, and mouse monoclonal anti-Hsp27 from Stressgen (San Diego, CA); and mouse monoclonal anti-actin from Sigma.

Cell Culture

A549 and HeLa cells were cultured in RPMI 1640 with 10% fetal bovine serum (FBS), 100 μg/ml streptomycin and 100 U/ml penicillin. *Hsp70*$^{-/-}$ and *Hsp70*$^{+/+}$ murine fibroblasts were cultured in DMEM-high glucose with 1 mM sodium pyruvate 10% FBS, 100 μg/ml streptomycin and 100 U/ml penicillin.

Transfections

HeLa cells were transfected with siRNA as previously described (23). Briefly, cells were plated in 6-well plates at a density of 5×10^5 cells per well and allowed to adhere for 20–24 h. Four hundred nmol of control siRNA #1 or Hsp70 specific siRNA (23) was complexed with 10 μl of Lipofectamine™ 2000 (Invitrogen) in 0.5 ml of Opti-MEM (Invitrogen) for 10 min. Cells were incubated for 4 hours with complexed lipid-siRNA, after which 1 ml of Opti-MEM containing 35% FBS was added. The next day, cultures were washed once with serum-free medium, and fresh medium was added. Cells were trypsinized and replated for clonogenic assays or immunoblotting the next day, as described below.

Clonogenic Assays

A549 cells, or HeLa cells transfected with control or Hsp70 specific siRNA, were trypsinized and plated in 60-mm tissue culture plates to a density of 1500 cells per plate. After cells were allowed to adhere for 22–24 hours, drugs were added as indicated to final concentrations from 100-fold concentrated stocks. After a 24 h incubation, plates were washed twice with serum-free medium, then incubated in fresh medium until colonies were visible. The plates were washed once with PBS, and stained with Coomassie brilliant blue. Visible colonies were counted, with typical plating efficiencies of 17–26%.

MTS assays

MTS assays were carried out using the CellTiter 96 Non-Radioactive Cell Proliferation Assay (Promega, Madison, WI) according to manufacturer's instructions. Briefly, cells were plated

in 96-well plates at a density of 500, 500, and 1000 cells for A549, *Hsp70*$^{-/-}$ and *Hsp70*$^{+/+}$ fibroblasts, respectively. After cells were allowed to adhere for 24 hours, drugs were added as indicated to final concentrations from 100-fold concentrated stocks. After a 24-h incubation, plates were washed twice with serum-containing medium, supplemented with fresh medium and incubated for 5 additional days. Dye and stop solutions were added as directed by the supplier. Cell survival was estimated by absorbance, which was read at 570 nm.

Immunoblotting

Cells were plated on 100-mm dishes, allowed to adhere for 22–24 h, then treated as described. Adherent cells were lifted from plates by scraping, combined with non-adherent cells, pelleted at 250 × g for 5 min at 4°C, rinsed once with ice-cold PBS and then lysed in lysis buffer containing 10 mM HEPES (pH 7.4), 20 mM sodium molybdate, 150 mM KCl, 10 mM $MgCl_2$, 0.1% Nonidet P-40, 1 mM Na_3VO_4, and protease inhibitors (Complete, mini, EDTA-free, tablets; Roche (Indianapolis, IN)). After a 10 min incubation on ice, the detergent insoluble fractions were pelleted at 18,000 × g for 2 min at 4°C. Total protein concentration of supernatants were estimated by the bicinchoninic acid (BCA) method (33). Aliquots containing 50 μg of protein were separated by one-dimensional SDS-PAGE, transferred to nitrocellulose, probed with antibodies and visualized by enhanced chemiluminescence as previously described (34).

Non-denaturing Gel Electrophoresis

Cells were treated as indicated, then harvested by scraping. Cells were washed once with ice-cold PBS, resuspended in Buffer A (10 mM Hepes (pH 7.9), 10 mM KCl, 0.1 mM EDTA, 0.1 mM EGTA, 100 μM DTT, 500 μM AEBSF), and incubated for 15 min on ice. Nonidet P-40 was then added to a final concentration of 0.2% (v/v). After each sample was vortexed, and sedimented at 14,000 rpm for 1 min, the supernatant was collected for cytoplasmic fraction. Nuclei were resuspended in ice-cold Buffer B (20 mM Hepes (pH 7.9), 25% glycerol, 0.4 M NaCl, 1 mM EDTA, 1 mM EGTA, 100 μM DTT, 500 μM AEBSF), vortexed for 20 min at 4° C, and sedimented at 14,000 rpm for 5 min. The supernatant was collected for nuclear fraction. The total protein concentrations of cytoplasmic and nuclear fractions were estimated by the bicinchoninic acid method (33). Aliquots containing 50 μg of protein were subjected to electrophoresis using 10% Ready Gel pre-cast gels and diluted Tris-Glycine buffer from Biorad (Hercules, CA). The separated proteins were transferred to nitrocellulose, probed with antibodies and visualized by enhanced chemiluminescence as previously described (34).

Hoechst 33258 Staining

Cells were treated for 24 h, washed and incubated in drug-free medium as indicated. Cells were harvested by scraping. Adherent and non-adherent cells were combined and pelleted at 250 × g for 5 min at 4°C, rinsed once with ice-cold PBS, and fixed in 3:1 methanol: acetic acid overnight at room temp. Fixed cells were applied to coverslips, then stained with 1 μg/ml Hoechst 33258 in 50 mM Tris-HCl (pH 7.4 at 21°C) containing 50% (v/v) glycerol. Apoptosis was determined by examining slides by fluorescence microscopy and recording the number of cells that demonstrated chromatin condensation or nuclear fragmentation. At least 500 cells were counted per slide.

Immunofluorescence

Cells were stained with the rabbit polyclonal anti-HSF-1 antibody according to He, *et al*. (35) with the following changes: A549 cells were plated on glass coverslips and allowed to adhere for 24 h. Cells were treated for 24 h with drugs as indicated, washed once with microtubule stabilizing buffer (3 mM EGTA, 50 mM PIPES, 1 mM $MgSO_4$, 25 mM KCl) and fixed in the wells with 4% paraformaldehyde in PBS (v/v) for 30 min at room temperature.

Cells were blocked for 1 h at 37°C in blocking buffer containing the following: 5% normal goat serum, 1% glycerol, 0.1% BSA, 0.1% fish skin gelatin, 0.04% sodium azide. Primary antibody was diluted in blocking buffer, then incubated with cells for 1 h at 37°C. After three washes in 1X PBS, cells were incubated with Alexa Fluor 568 goat anti-rabbit IgG (Invitrogen) for 1 h at 37°C, washed with PBS then fixed for an additional 5 min in 4% PFA at room temp. Images were captured using a 100X oil objective on a Zeiss LSM 510 Confocal Laser Scanning Microscope.

Reverse Transcriptase-PCR

RNA was harvested from cells using the RNeasy kit from Qiagen (Valencia, CA). 250 ng RNA was used for each condition, then one-step RT-PCR was carried out using SuperScript One-Step RT-PCR with Platinum Taq from Invitrogen (Carlsbad, CA) according to manufacturer's instructions. Primers were as follows: Hsp90 forward: 5′-GCCTCTGGTGATGAGATGGT-3′, and reverse: 5′-CATGGAGATGTCACCAATCG-3′; Hsp70 forward: 5′-CGACCTGAACAAGAGCATCA-3′, and reverse: 5′-AAGATCTGCGTCTGCTTGGT-3′; Hsp27 forward: 5′-GGACGAGCATGGCTACATCT-3′, and reverse: 5′-GACTGGGATGGTGATCTCGT-3′; p21 forward: 5′-GACACCACTGGAGGGTGACT-3′, and reverse: 5′-CAGGTCCACATGGTCTTCCT-3′. Conditions for RT-PCR were as follows: 1 cycle of 50°C for 30 min, then 25 cycles of 94°C for 15 sec, 60°C for 30 sec, and 72°C for 60 sec, followed by 1 cycle of 72°C for 5 min.

Chromatin Immunoprecipitation (ChIP)

ChIP was carried out using the Chromatin Immunoprecipitation Assay Kit from Millipore (Billerica, MA) according to manufacturer's instructions. Briefly, 15–20 million cells were cultured for each condition. After drug treatment, cells were washed and placed in fresh medium. DNA crosslinks were formed by adding formaldehyde to medium to a final concentration of 1% (v/v) and incubating for 10 min at 37°C. Cells were then washed, harvested by scraping, lysed on ice for 10 min using the kit SDS lysis buffer, and sonicated with 5 pulses at maxium power to shear DNA, with 1 min cooling between each 8 sec pulse. After lysates were cooled on ice for 3 min and sedimented at 14,000 rpm for 10 min, the supernatant was diluted to 1 ml with ChIP dilution buffer from the kit. Lysates were precleared at 4°C for 1 hour using Protein-A Sepharose beads (Sigma). Lysates were then rotated with HSF-1 polyclonal antibody (Stressgen) overnight at 4°C, supplemented with the beads from the kit, and rotated overnight again at 4°C. After beads were washed as directed, crosslinks were reversed as indicated in the kit directions. DNA was precipitated using phenol-chloroform extraction followed by ethanol precipitation. PCR to amplify the HSE DNA bound to HSF-1 was carried out using PCR supermix (Invitrogen) with the following primers that result in an approximately 183 bp band: forward: 5′-GAAGACTCTGGAGAGTTCTG-3′, and reverse: 5′-CCCTGGGCTTTTATAAGTCG-3′ (primer sequences provided by Dr. Richard Morimoto).

Statistical analysis

Statistical analysis consisted of the two-tailed paired *t* test. A p-value of < 0.05 indicated statistical significance. Synergy for clonogenic assays was determined by the median effect method. In brief, cells were treated with serial dilutions of each drug individually and with both drugs simultaneously or sequentially at a fixed ratio of doses. The fractional survival (*f*) was calculated by dividing the number of colonies in drug-treated plates by the number of colonies in control plates. Log $[(1/f) - 1]$ was plotted against log [drug dose]. From the resulting graphs, the *x* intercept (log IC_{50}) and slope *m* were calculated for each drug and for the combination by the method of least squares and then used to calculate the doses of the individual drugs and the combination required to produce varying levels of cytotoxicity, then the CI was then calculated using the Calcusyn program (Biosoft, Cambridge, UK) (36).

Results

Combination of Hsp90-directed agents and cisplatin are synergistic

To examine the potential effect of combining GA and CDDP *in vitro*, we performed clonogenic assays using A549 cells. We compared the cytotoxicity of the GA + CDDP combination to the effect of the two agents alone using the median effect method (36), which determines whether the cytotoxicity for the combination is greater than (CI < 1), equal to (CI = 1), or less than (CI > 1) the additive effect of the individual agents. For these experiments we used the ratio of 1:20: of GA:CDDP as determined by the ratio of the IC_{50} for each agent in A549 cells.

Our data indicated that simultaneous exposure to GA or 17-AAG and CDDP resulted in synergistic antiproliferative effects, especially at doses near the IC_{50} for 17-AAG+CDDP and IC_{90} for GA+CDDP (CI=0.549 ± 0.197 and 0.296 ± 0.134, respectively, Figure 1A) but not at low concentrations. Subsequently, we examined A549 cells treated continuously with DMSO (control), 100 nM GA, 30 μM CDDP, or 100 nM and 30 μM CDDP for apoptotic nuclear changes. After Hoechst 33258 staining, more nuclear fragmentation was evident in cells treated with the combination treatment as compared to either GA or CDDP alone at 72, 96, and 120 h (Figure 1B). From these data we conclude that the synergy observed when GA is combined with CDDP is consistent with enhanced cell death due to combination treatment.

CDDP blocks induction of stress-responsive proteins

To examine the mechanistic basis for this synergistic interaction, we determined the effect of CDDP on the stress response, which is an important determinant of sensitivity to GA and 17AAG. When lysates from cells collected for Hoechst staining were examined for stress-inducible proteins, the increased expression of Hsp70 and Hsp27 observed after GA treatment (Figure 2A, lanes 2, 6, 10), was much less prominent after CDDP (lanes 3, 7, 11) or the combination treatment (lanes 4, 8, 12). These data suggested that treatment with CDDP prevented upregulation of stress-inducible proteins that occurs after GA treatment. To better define the dose dependence of the CDDP-mediated block of the heat shock response during GA treatment, lysates from cells treated for 24 h with DMSO (Figure 2B, lanes 1, 7), GA alone (lanes 2 and 8), increasing doses of CDDP (lanes 9–12), or GA and increasing CDDP (lanes 3–6), were blotted for stress-inducible proteins. As shown in Figure 2B, CDDP blocked the induction of Hsp70 and Hsp27 by GA during simultaneous treatment even at doses as low as 3 μM. Interestingly, after treatment with CDDP we observed a mobility shift for HSF-1 that is often associated with phosphorylation (Figure 2B). It is notable that the most extreme mobility shift for HSF-1 occurred at the highest dose of CDDP even without GA present, suggesting that phosphorylation might be responsible for the decreased HSF-1-mediated transcription after treatment with the combination (37).

To determine whether the decreased Hsp70 and Hsp27 protein levels observed after combination treatment reflected a decrease in the mRNAs, we performed reverse-transcriptase PCR (RT-PCR) using total mRNA collected from cells treated with DMSO, GA, CDDP or GA combined with increasing doses of CDDP. As shown in Figure 2C, Hsp90β transcription remained steady with GA, CDDP or combination treatment. Treatment with CDDP abrogated the transcription of Hsp70 and Hsp27 at 3, 10, and 30 μM, (lanes 6, 7, 8, respectively). Conversely, treatment with CDDP increased transcription of p21, a cell cycle regulator that is transcriptionally regulated by p53 after DNA-damaging chemotherapy, including CDDP (38). These data demonstrate that CDDP causes decreased transcription of stress-inducible HSE-containing genes that are upregulated during GA treatment, but not other genes such as Hsp90β and p21, suggesting that CDDP-induced downregulation of HSE-containing genes is unlikely to be due to decreased global cellular transcription.

Hsp70 contributes to resistance to Hsp90-directed agents

Because the combination treatment caused a decrease in stress-responsive proteins such as Hsp70 and Hsp27, two proteins previously implicated in 17-AAG resistance (21,23), we assessed whether blocking the induction of Hsp70 would contribute to greater 17-AAG sensitivity. When HeLa cells transfected with Hsp70 siRNA, were treated with 17-AAG for 24 h and examined using colony-forming assays, a 3-fold decrease in IC_{50} was observed relative to control transfected cells (IC_{50} = 23.4 ± 11.7 nM and 85.0 ± 32.0 nM, respectively, Figure 3A). Likewise, MTS assays demonstrated that the IC_{50} of mouse embryonic fibroblasts lacking *Hsp70* (*Hsp70*$^{-/-}$) is at least 10-fold lower than in isogenic cells containing *Hsp70* (*Hsp70*$^{+/+}$) (Figure 3B, IC_{50} = 4.3 ± 2.9 nM and 63.7 ± 14.9 nM, respectively) (19). Interestingly, MTS assays also revealed that the IC_{50} of *Hsp70*$^{-/-}$ cells treated with CDDP alone or GA + CDDP are not significantly different (Figure 3C, IC_{50} = 365 ± 130 nM and 180 ± 144 nM, respectively, $p < 0.37$) consistent with CDDP effect being mediated in part by abrogation of the heat shock response. Together, these data indicate that Hsp70 contributes to GA resistance, and imply that blocking Hsp70 induction through inhibition of HSF-1 action might increase GA sensitivity.

GA causes HSF-1 activation in the presence of CDDP

Previous studies have implicated HSF-1-regulated transcription in the heat shock response (10,12,30,31). Many steps are required for HSF-1 activation, including phosphorylation, trimerization and localization to the nucleus, where HSF-1 binds to DNA containing HSE promoters. Our data, combined with work by Bagatell, *et al*., suggest that CDDP blocks HSF-1-induced upregulation of heat shock proteins after GA treatment (39). However, the precise mechanism for this decrease in stress-inducible proteins has not been addressed to date. We first assessed whether HSF-1 trimerized after treatment. Non-denaturing gel electrophoresis followed by immunoblotting was used to examine the oligomeric state of HSF-1 in cells treated with DMSO, 100 nM GA, 30 μM CDDP, or GA and CDDP simultaneously. As indicated in Figure 4A, HSF-1 was present in both monomeric and trimeric forms in the cytoplasmic portion of cells, with less monomer occurring in cells treated with either GA or GA+CDDP (left panel, lanes 2 and 4, respectively, Figure 4A). However, CDDP alone did not cause a loss of the monomer (left panel, lane 3, Figure 4A). Strikingly, an accumulation of the trimerized form of HSF-1 was found within the nuclear fractions in cells treated with GA or GA+CDDP (middle panel, lanes 2 and 4, respectively, Figure 4A), which indicated activation and nuclear localization. This accumulation of trimerized HSF-1 in the nucleus explained the decrease of the monomeric form in the cytoplasmic fraction. To control for loading, the fractions were combined to show total protein for each treatment (right panel, Figure 4A). These data demonstrate that HSF-1 was trimerized, and thereby potentially activated, in the presence of GA + CDDP despite the observed decrease in stress-responsive gene transcription versus GA alone.

Next we examined whether HSF-l forms nuclear stress granules after treatment with GA, CDDP, or GA + CDDP (27,28). Immunofluorescent staining for HSF-1 revealed that no stress granules could be observed in cells treated with DMSO or CDDP (Figure 4B, left panels). Conversely, treatment with GA or GA + CDDP resulted in stress granule formation, shown as punctate staining in the cell nucleus (Figure 4B, right panels, white arrows). Taken together, our data indicate that CDDP is able to block GA-induced transcription of stress response genes such as Hsp70 and Hsp27, but does not appear to block HSF-1 trimerization or localization to nuclear stress granules.

Cisplatin blocks HSF-1 binding to chromatin

Based on the preceding results, we hypothesized that CDDP might affect HSF-1 binding to DNA. To assess whether HSF-1 can bind HSE sequences in cells treated with CDDP, we

performed chromatin immunoprecipitation. Immunoprecipitated HSF-1 from untreated cells or cells treated with DMSO or CDDP had low binding to the HSE (Figure 4C, lanes 4, 6, respectively). As expected, treatment with GA increased binding compared to DMSO alone (lane 5). Strikingly, HSF-1 chromatin binding is decreased in cells treated with GA + CDDP versus GA alone (Figure 4C, lanes 7 and 5, respectively). These data are consistent with CDDP inhibiting HSF-1 binding to HSE-containing DNA, even in the presence of GA.

Melphalan, but not camptothecin, blocks GA-induced stress response upregulation

In further experiments, we examined the effect of combining GA with the DNA crosslinking agent melphalan (MEL) or the topoisomerase I poison camptothecin (CPT). Both of these drugs can block transcription and cause cancer cell death (40,41). MTS assays showed that GA increased the cell death observed with both MEL and CPT (Figure 5A, B). For MEL the IC_{50} decreased from 103 ± 29.1 nM in the absence of GA to 10.5 ± 12.2 nM in the presence of GA. For CPT, the IC_{50} decreased from 303.4 ± 90.2 nM in the absence of GA to 98.7 ± 53.8 nM in the presence of GA. Western blotting revealed that Hsp70 upregulation is blocked in a dose-dependent manner when MEL is added to GA (Figure 5C, lanes 5 and 6). Conversely, CPT did not block Hsp70 upregulation as dramatically as MEL, even at high doses (Figure 5C, lanes 7 and 8). These data suggest that abrogation of stress response induction by MEL may cause added cell death when it is combined with GA. CPT, on the other hand, appears to increase cell killing when combined with GA through mechanisms other than abrogation of HSF-1-mediated transcription. This conclusion agrees with studies by Flatten, *et al*. which demonstrated 17-AAG and CPT derivative SN-38 were synergistic when combined, and concluded that this synergy resulted from downregulation of Chk1 (42).

Discussion

Previous studies have yielded somewhat conflicting results when 17-AAG and CDDP were combined in various cell types. Vasilevskaya, *et al*. initially reported additive effects when cisplatin was combined with 17-AAG, although the combination was even found to be antagonistic in some cell lines (8,17). Variations between cell lines were reported to result from differential caspase activation, possibly attributable to differences in p53-mediated stimulation of apoptosis after treatment. In contrast, Bagatell, *et al*. reported synergistic effects in neuroblastoma and osteosarcoma cell lines when 17-AAG was combined with CDDP (39). Likewise, our data show that the combination of 17-AAG and CDDP is synergistic *in vitro* using non-small cell lung cancer cell line A549. Quantitation of apoptotic cells (Figure 1B) indicates increased cell killing by the combination.

Previous studies have implicated Hsp70 (21,22) and Hsp27 (23) in resistance to 17-AAG. Our experiments demonstrated that CDDP, when combined with 17-AAG, could block HSF-1-induced Hsp70 upregulation (Figure 2), in agreement with the results of Bagatell, *et al*. (39). Furthermore, we show that CDDP blocks the upregulation of Hsp27, another HSE-regulated gene, while still causing upregulation of p21, a gene that is increased in response to p53 activation after CDDP treatment (38). The survival data (Figure 3) showing that Hsp70 knockdown and lack of effect on CDDP sensitivity in the *Hsp70*$^{-/-}$ cells further support that CDDP is affecting the heat shock response. The relatively selective inhibition of GA-induced Hsp70 and Hsp27 induction provides a plausible explanation for the observed synergy between CDDP and GA or 17-AAG.

There are several possible mechanisms by which CDDP could block HSF-1 activity. First, CDDP could crosslink HSF-1 to the Hsp90 chaperone complex, which would sequester HSF-1 as an inactive monomer, thereby repressing its transcriptional activity. A previous study demonstrated that treatment with GA + CDDP resulted in high-molecular weight crosslinked Hsp90 (39). It was unclear from that study whether HSF-1 is contained in these complexes.

Our results indicate by two separate criteria that HSF-1 is activated in response to GA + CDDP treatment (figure 4). These observations suggest that HSF-1 has been released from Hsp90 as a result of GA treatment and that CDDP is interfering downstream of this activation. It is important to note that the synergistic interaction between GA and CDDP is observed only at higher concentrations which may reflect a concentration dependent effect of CDDP on the heat shock response. However, the effects of CDDP on HSF-1-mediated upregulation of stress-responsive genes were studied using concentrations that caused synergistic cell killing.

In further experiments, we demonstrated that CDDP interferes with HSF-1 binding to DNA. This could occur through adduct formation on HSF-1 or the HSE-containing DNA. First, CDDP binding could prevent HSF-1 trimerization or interfere with HSF-1 DNA binding activity. This would thereby block the induction of HSE-containing genes. Second, CDDP has been shown to preferentially bind to guanine and adenine nucleotides (43). Since HSEs are known to contain G-A rich consensus sequences composed of inverted repeats of the pentamer 5′-nGAAn-3′ (29–31), CDDP may be stochastically more likely to bind to the HSE promoter, resulting in semi-selective inhibition of stress-responsive protein upregulation. By causing DNA adducts in this region, CDDP could act as a direct steric hindrance for HSF-1 binding to the promoter element, thereby causing decreased transcription of stress-responsive genes.

Another possibility is that CDDP is affecting upstream signaling events that modulate HSF-1 activity. HSF-1 phosphorylation is a key regulator of transcriptional activity. To date, phosphorylation at two sites, Thr142 and Ser230, has been shown to increase transcriptional activity of HSF-1 up to 3-fold (37). Our data suggest that CDDP treatment is inducing phosphorylation of HSF-1 (Figure 2B), which could indicate activation. However, it is possible that CDDP is stimulating the phosphorylation of one or more of the other known sites on HSF-1, including Ser121, Ser303, Ser307, Ser326, and Ser363, which decrease HSF-1 activity (37). Interestingly, a study by Vasilevskaya, *et al*. demonstrated that inhibition of JNK kinase increased survival after treatment with GA + CDDP, and that constitutively active JNK signaling pathways were sufficient to increase cytotoxicity of the GA+CDDP combination (44). Since JNK was previously shown to phosphorylate HSF-1 on Ser363, which inhibits transcriptional activity (37), it is possible that CDDP may be causing JNK-induced HSF-1 phosphorylation, resulting in decreased transcriptional activation. This decrease in transcription could in turn prevent upregulation of stress-responsive proteins such as Hsp70, which has been correlated with resistance to both 17-AAG and CDDP (10,12,20).

Our studies have raised another possibility for pharmacologic manipulation to enhance 17-AAG activity. Hsp70 and Hsp27 have been previously implicated in resistance to Hsp90-directed agents (21–23). Targeting these proteins directly could represent a new strategy for increasing 17-AAG efficacy. Alternatively, targeting the upregulation of these proteins through inhibition of stress response-induced transcription could provide even greater sensitivity to Hsp90-directed therapy. Although agents that block the stress response, such as quercetin and KNK437 exist (12), neither is a specific inhibitor of HSF-1. Therefore, identifying new compounds that specifically inhibit HSF-1 activity while maintaining low toxicity may be the key to promoting 17-AAG as an effective therapy for cancer treatment. Until then, it may be possible to enhance the cytotoxicity of 17-AAG in the clinic with standard chemotherapeutics such as CDDP or MEL that can block, at least partially, the HSF-1-mediated heat shock response that occurs after treatment with Hsp90-targeted agents.

Acknowledgements

National Cancer Institute Grants CA90390 and CA15083 and a predoctoral fellowship from the Mayo Foundation (A.K. McCollum, K.B. Lukasiewicz).

We would like to thank Dr. Tej K. Pandita for providing *Hsp70*$^{-/-}$ and *Hsp70*$^{+/+}$ cell lines, Drs. Scott Kaufmann and Larry Karnitz for scientific discussion and critical reading of the manuscript, and Dr. Martin Fernandez-Zapico for assistance with the ChIP assay.

Abbreviations

Hsp90
heat shock protein 90

GA
geldanamycin

17-AAG
17-allylaminogeldanamycin

HSF-1
heat shock factor-1

HSE
heat shock element

CDDP
cisplatin

Hsp70
heat shock protein 70

Hsp27
heat shock protein 27

BCA
bicinchoninic acid

ChIP
chromatin immunoprecipitation

CI
combination index

DMSO
dimethyl sulfoxide

MEL
melphalan

CPT
camptothecin

JNK
Jun N-terminal kinase

References

1. Pearl LH, Prodromou C. Structure and mechanism of the Hsp90 molecular chaperone machinery. Annu Rev Biochem 2006;75:271–94. [PubMed: 16756493]
2. Obermann WM, Sondermann H, Russo AA, Pavletich NP, Hartl FU. In vivo function of Hsp90 is dependent on ATP binding and ATP hydrolysis. J Cell Biol 1998;143:901–10. [PubMed: 9817749]

3. Prodromou C, Roe SM, O'Brien R, Ladbury JE, Piper PW, Pearl LH. Identification and structural characterization of the ATP/ADP-binding site in the Hsp90 molecular chaperone. Cell 1997;90:65–75. [PubMed: 9230303]
4. Stebbins CE, Russo AA, Schneider C, Rosen N, Hartl FU, Pavletich NP. Crystal structure of an Hsp90-geldanamycin complex: targeting of a protein chaperone by an antitumor agent. Cell 1997;89:239–50. [PubMed: 9108479]
5. Grenert JP, Sullivan WP, Fadden P, et al. The amino-terminal domain of heat shock protein 90 (hsp90) that binds geldanamycin is an ATP/ADP switch domain that regulates hsp90 conformation. J Biol Chem 1997;272:23843–50. [PubMed: 9295332]
6. Whitesell L, Mimnaugh EG, De Costa B, Myers CE, Neckers LM. Inhibition of heat shock protein HSP90-pp60v-src heteroprotein complex formation by benzoquinone ansamycins: essential role for stress proteins in oncogenic transformation. Proc Natl Acad Sci U S A 1994;91:8324–8. [PubMed: 8078881]
7. Neckers L. Chaperoning oncogenes: Hsp90 as a target of geldanamycin. Handb Exp Pharmacol 2006:259–77. [PubMed: 16610363]
8. Goetz MP, Toft DO, Ames MM, Erlichman C. The Hsp90 chaperone complex as a novel target for cancer therapy. Ann Oncol 2003;14:1169–76. [PubMed: 12881371]
9. Kamal A, Boehm MF, Burrows FJ. Therapeutic and diagnostic implications of Hsp90 activation. Trends Mol Med 2004;10:283–90. [PubMed: 15177193]
10. Whitesell L, Bagatell R, Falsey R. The stress response: implications for the clinical development of hsp90 inhibitors. Curr Cancer Drug Targets 2003;3:349–58. [PubMed: 14529386]
11. Winklhofer KF, Reintjes A, Hoener MC, Voellmy R, Tatzelt J. Geldanamycin restores a defective heat shock response in vivo. J Biol Chem 2001;276:45160–7. [PubMed: 11574536]
12. Powers MV, Workman P. Inhibitors of the heat shock response: biology and pharmacology. FEBS Lett 2007;581:3758–69. [PubMed: 17559840]
13. Kim HR, Kang HS, Kim HD. Geldanamycin induces heat shock protein expression through activation of HSF1 in K562 erythroleukemic cells. IUBMB Life 1999;48:429–33. [PubMed: 10632574]
14. Whitesell L, Shifrin SD, Schwab G, Neckers LM. Benzoquinonoid ansamycins possess selective tumoricidal activity unrelated to src kinase inhibition. Cancer Res 1992;52:1721–8. [PubMed: 1551101]
15. Uehara Y, Hori M, Takeuchi T, Umezawa H. Phenotypic change from transformed to normal induced by benzoquinonoid ansamycins accompanies inactivation of p60src in rat kidney cells infected with Rous sarcoma virus. Mol Cell Biol 1986;6:2198–206. [PubMed: 3023921]
16. Supko JG, Hickman RL, Grever MR, Malspeis L. Preclinical pharmacologic evaluation of geldanamycin as an antitumor agent. Cancer Chemother Pharmacol 1995;36:305–15. [PubMed: 7628050]
17. Nowakowski GS, McCollum AK, Ames MM, et al. A phase I trial of twice-weekly 17-allylamino-demethoxy-geldanamycin in patients with advanced cancer. Clin Cancer Res 2006;12:6087–93. [PubMed: 17062684]
18. Smith V, Hobbs S, Court W, Eccles S, Workman P, Kelland LR. ErbB2 overexpression in an ovarian cancer cell line confers sensitivity to the HSP90 inhibitor geldanamycin. Anticancer Res 2002;22:1993–9. [PubMed: 12174876]
19. Munster PN, Basso A, Solit D, Norton L, Rosen N. Modulation of Hsp90 function by ansamycins sensitizes breast cancer cells to chemotherapy-induced apoptosis in an RB- and schedule-dependent manner. Clin Cancer Res 2001;7:2228–36. [PubMed: 11489796]
20. Schmitt E, Gehrmann M, Brunet M, Multhoff G, Garrido C. Intracellular and extracellular functions of heat shock proteins: repercussions in cancer therapy. J Leukoc Biol 2007;81:15–27. [PubMed: 16931602]
21. Guo F, Rocha K, Bali P, et al. Abrogation of heat shock protein 70 induction as a strategy to increase antileukemia activity of heat shock protein 90 inhibitor 17-allylamino-demethoxy geldanamycin. Cancer Res 2005;65:10536–44. [PubMed: 16288046]
22. Schmitt E, Maingret L, Puig PE, et al. Heat shock protein 70 neutralization exerts potent antitumor effects in animal models of colon cancer and melanoma. Cancer Res 2006;66:4191–7. [PubMed: 16618741]

23. McCollum AK, Teneyck CJ, Sauer BM, Toft DO, Erlichman C. Up-regulation of heat shock protein 27 induces resistance to 17-allylamino-demethoxygeldanamycin through a glutathione-mediated mechanism. Cancer Res 2006;66:10967–75. [PubMed: 17108135]
24. Bagatell R, Paine-Murrieta GD, Taylor CW, et al. Induction of a heat shock factor 1-dependent stress response alters the cytotoxic activity of hsp90-binding agents. Clin Cancer Res 2000;6:3312–8. [PubMed: 10955818]
25. Zou J, Guo Y, Guettouche T, Smith DF, Voellmy R. Repression of heat shock transcription factor HSF1 activation by HSP90 (HSP90 complex) that forms a stress-sensitive complex with HSF1. Cell 1998;94:471–80. [PubMed: 9727490]
26. Shi Y, Mosser DD, Morimoto RI. Molecular chaperones as HSF1-specific transcriptional repressors. Genes Dev 1998;12:654–66. [PubMed: 9499401]
27. Sandqvist A, Sistonen L. Nuclear stress granules: the awakening of a sleeping beauty? J Cell Biol 2004;164:15–7. [PubMed: 14709538]
28. Cotto J, Fox S, Morimoto R. HSF1 granules: a novel stress-induced nuclear compartment of human cells. J Cell Sci 1997;110 (Pt 23):2925–34. [PubMed: 9359875]
29. Voellmy R. On mechanisms that control heat shock transcription factor activity in metazoan cells. Cell Stress Chaperones 2004;9:122–33. [PubMed: 15497499]
30. Cotto JJ, Morimoto RI. Stress-induced activation of the heat-shock response: cell and molecular biology of heat-shock factors. Biochem Soc Symp 1999;64:105–18. [PubMed: 10207624]
31. Lindquist S. The heat-shock response. Annu Rev Biochem 1986;55:1151–91. [PubMed: 2427013]
32. Barent RL, Nair SC, Carr DC, et al. Analysis of FKBP51/FKBP52 chimeras and mutants for Hsp90 binding and association with progesterone receptor complexes. Mol Endocrinol 1998;12:342–54. [PubMed: 9514152]
33. Smith PK, Krohn RI, Hermanson GT, et al. Measurement of protein using bicinchoninic acid. Anal Biochem 1985;150:76–85. [PubMed: 3843705]
34. Kaufmann SH. Reutilization of immunoblots after chemiluminescent detection. Anal Biochem 2001;296:283–6. [PubMed: 11554725]
35. He B, Meng YH, Mivechi NF. Glycogen synthase kinase 3beta and extracellular signal-regulated kinase inactivate heat shock transcription factor 1 by facilitating the disappearance of transcriptionally active granules after heat shock. Mol Cell Biol 1998;18:6624–33. [PubMed: 9774677]
36. Chou TC, Talalay P. Quantitative analysis of dose-effect relationships: the combined effects of multiple drugs or enzyme inhibitors. Adv Enzyme Regul 1984;22:27–55. [PubMed: 6382953]
37. Holmberg CI, Tran SE, Eriksson JE, Sistonen L. Multisite phosphorylation provides sophisticated regulation of transcription factors. Trends Biochem Sci 2002;27:619–27. [PubMed: 12468231]
38. Fan S, el-Deiry WS, Bae I, et al. p53 gene mutations are associated with decreased sensitivity of human lymphoma cells to DNA damaging agents. Cancer Res 1994;54:5824–30. [PubMed: 7954409]
39. Bagatell R, Beliakoff J, David CL, Marron MT, Whitesell L. Hsp90 inhibitors deplete key anti-apoptotic proteins in pediatric solid tumor cells and demonstrate synergistic anticancer activity with cisplatin. Int J Cancer 2005;113:179–88. [PubMed: 15455381]
40. Pieper RO, Futscher BW, Erickson LC. Transcription-terminating lesions induced by bifunctional alkylating agents in vitro. Carcinogenesis 1989;10:1307–14. [PubMed: 2736721]
41. Stewart AF, Schutz G. Camptothecin-induced in vivo topoisomerase I cleavages in the transcriptionally active tyrosine aminotransferase gene. Cell 1987;50:1109–17. [PubMed: 2887294]
42. Flatten K, Dai NT, Vroman BT, et al. The role of checkpoint kinase 1 in sensitivity to topoisomerase I poisons. J Biol Chem 2005;280:14349–55. [PubMed: 15699047]
43. Trimmer EE, Essigmann JM. Cisplatin. Essays Biochem 1999;34:191–211. [PubMed: 10730196]
44. Vasilevskaya IA, Rakitina TV, O'Dwyer PJ. Quantitative effects on c-Jun N-terminal protein kinase signaling determine synergistic interaction of cisplatin and 17-allylamino-17-demethoxygeldanamycin in colon cancer cell lines. Mol Pharmacol 2004;65:235–43. [PubMed: 14722256]

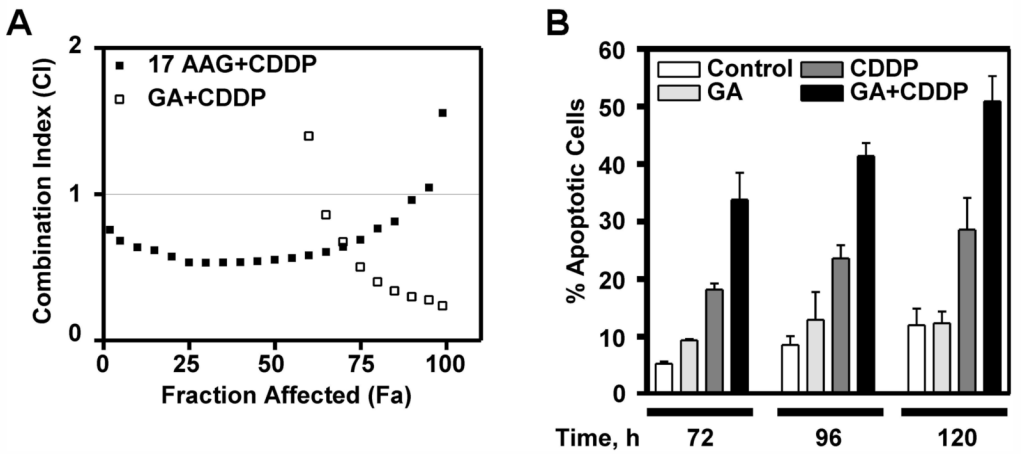

Figure 1.

GA+CDDP is synergistic. A: A549 cells were treated with vehicle (DMSO), 17-AAG, GA, CDDP, 17-AAG+CDDP, or GA+CDDP. After 24 h treatment, cells were washed, then incubated in fresh medium for 7 days to allow colony formation. Final DMSO concentration was 1% in all experiments. Using the median effect method, CI was determined for combinations. Fraction affected indicates fraction killed with treatment. CI=1, CI<1, and CI>1 indicates additivity, synergy, and antagonism of the combination, respectively. B: Cells were treated as indicated for 24 h, then washed and fresh medium was added. Cells were harvested at times indicated after initial treatment, then apoptotic morphology was observed, n=3 and error bars indicate ± SEM.

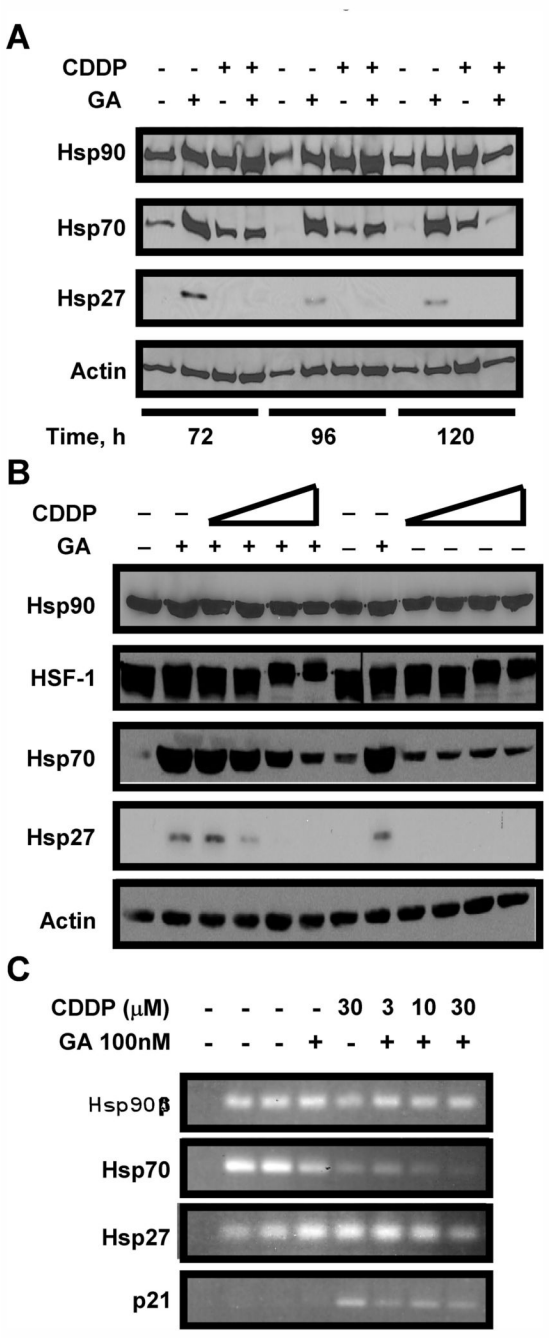

Figure 2.

A: CDDP abrogates HSF-1-mediated induction of Hsp70 and Hsp27. A: A549 cells were treated with vehicle (DMSO), 100 nM GA, 30 μM CDDP, or GA+CDDP 24 h, then washed, and incubated for times indicated from initial treatment. 50 μg of cell lysate was separated by SDS-PAGE, then probed by western blotting. Actin was used as a loading control. B: A549 cells were treated with vehicle (DMSO, lanes 1, 7), 100 nM GA, with or without increasing doses of CDDP for 24 h. 50 μg of cell lysate was separated by SDS-PAGE, then probed by western blotting. Actin is used as a loading control. C: 250 ng total mRNA from cells treated as indicated was amplified by one step RT-PCR, then separated on a 1% agarose gel. Lane 1: PCR reaction in absence of DNA, lane 2: untreated cells, lane 3: cells treated with DMSO.

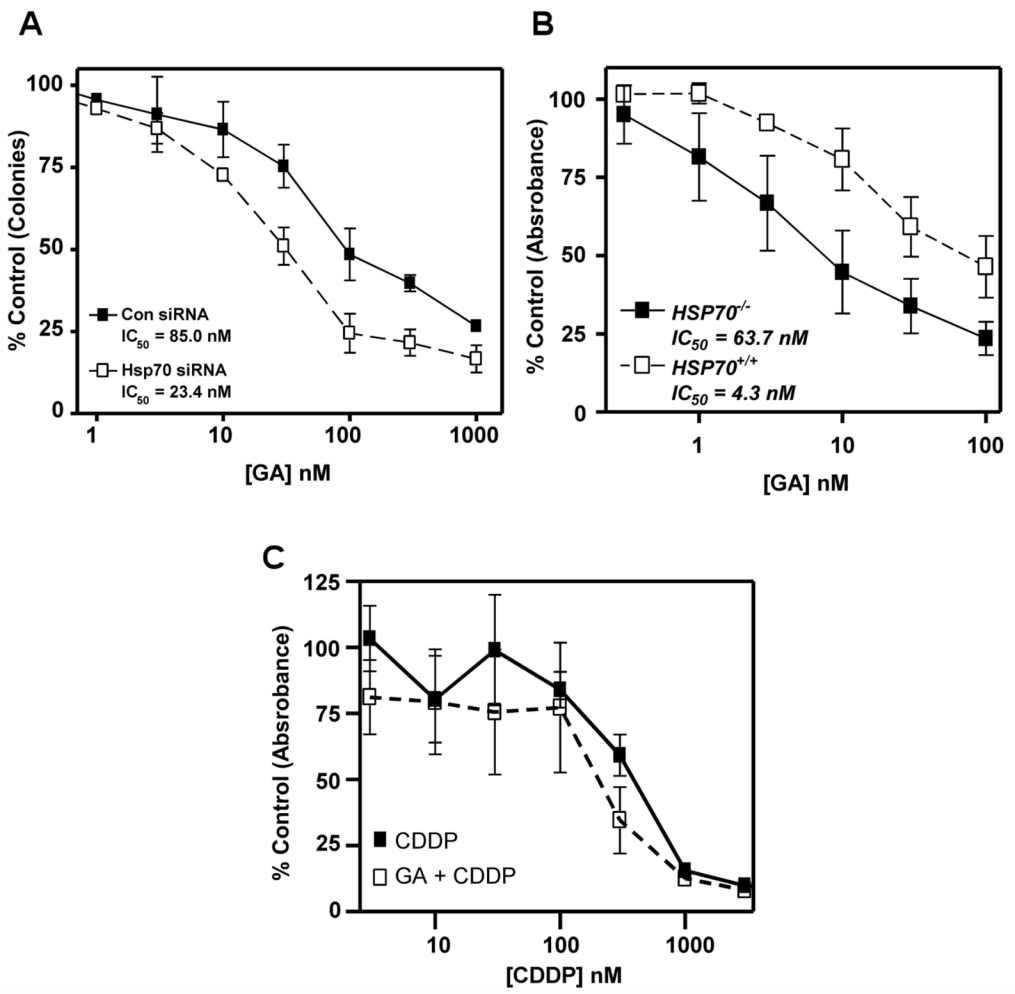

Figure 3.

Hsp70 contributes to Hsp90-directed therapy resistance. A: HeLa cells were transfected with control or Hsp70 siRNA as indicated, then plated for clonogenic assays. Cells were treated with GA for 24 h in concentrations indicated, then washed in serum-free medium and incubated in drug-free medium for 7 days to allow colonies to form. Error bars represent ± SEM, n=3. B: *Hsp70*$^{+/+}$ and *Hsp70*$^{-/-}$ were plated for MTS assays, treated with vehicle (DMSO) or GA for 24 h in concentrations indicated, then washed and incubated in drug-free medium for 3 days. Absorbance was read to determine number of surviving cells. Error bars indicate ± SEM, n=3. C: *Hsp70*$^{-/-}$ were plated for MTS assays, treated with CDDP or 4 nM GA + CDDP in concentrations indicated for 24 h, then washed and incubated in drug-free medium for 3 days. Absorbance was read to determine number of surviving cells. Error bars indicate ± SEM, n=5.

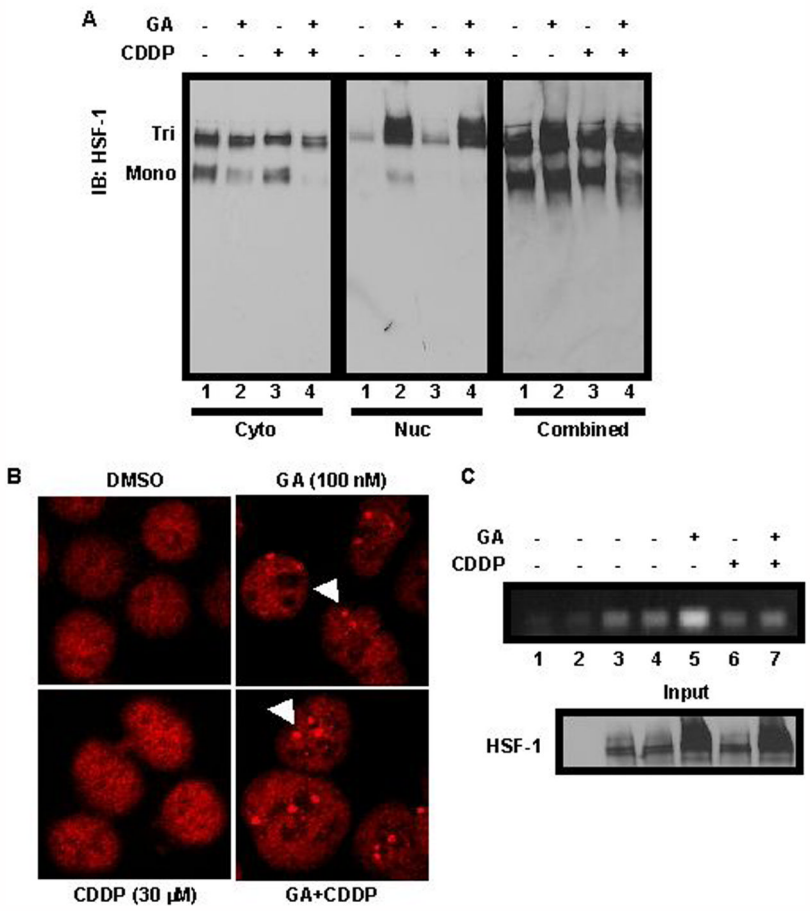

Figure 4.

CDDP blocks HSF-1 binding to chromatin. A: A549 cells were treated with vehicle (DMSO), 100 nM GA, 30 μM CDDP, or GA+CDDP for 24 h, then harvested and separated by non-denaturing PAGE. Western blotting was performed using 50 μg of cell lysates. Tri = HSF-1 trimer, Mono = HSF-1 monomer. Cytoplasmic (cyto) and nuclear (nuc) fractions were run separately as indicated, and combined to show total protein loading. B: A549 cells were treated with vehicle (DMSO), GA, CDDP, or GA+CDDP as indicated, then stained with HSF-1 antibody (red). Nuclear stress granules are indicated by white arrows. C: Upper: A549 cells were untreated (lane 3), or treated with vehicle (DMSO, lane 4), 100 nM GA (lane 5), 30 μM CDDP (lane 6), or GA+CDDP (lane 7) for 2 h, then cells were harvested and HSF-1-DNA crosslinks were immunoprecipitated (IP) from equal amounts of lysate. After PCR, amplified DNA was run on a 1.5% agarose gel. Lower: Protein eluted from IP probed for HSF-1 by western blotting is used as a loading control (Input).

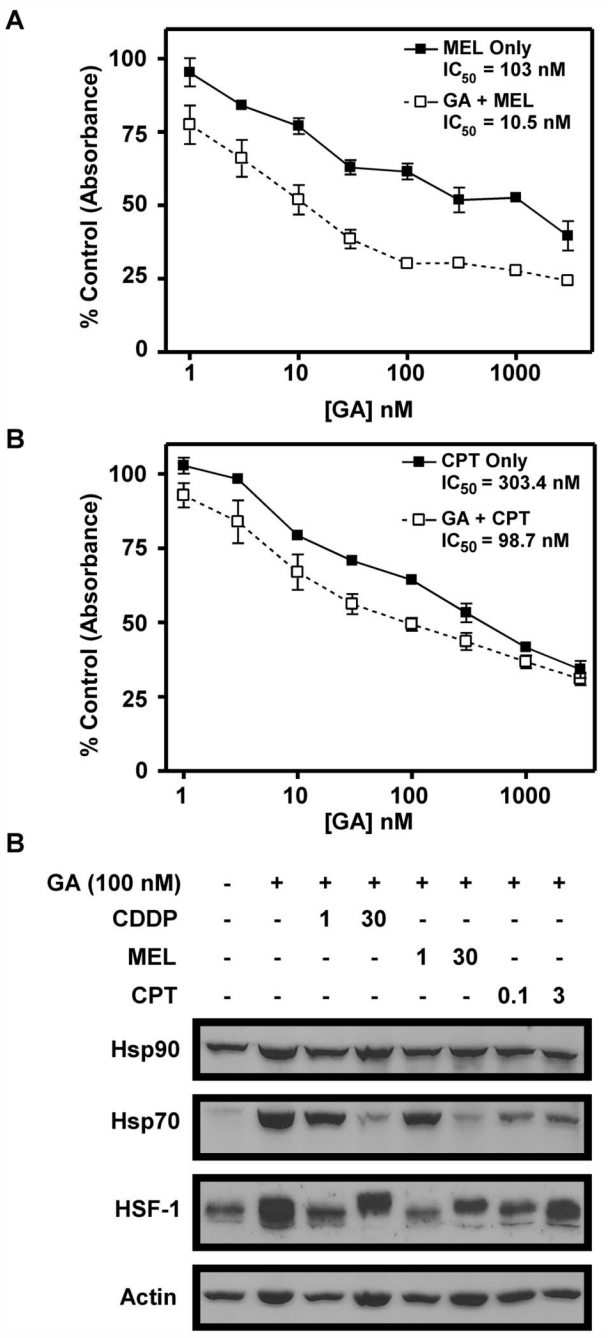

Figure 5.

Mel, but not CPT, blocks HSF-1-mediated transcription. A, B: A549 cells were treated with Mel, 100 nM GA+Mel, CPT, or 100 nM GA+CPT in doses indicated. Cells were treated for 24 h, then washed and incubated for 3 days in drug-free medium. Cell survival was estimated using MTS assay and measuring absorbance. C: A549 cells were treated with vehicle (DMSO, lane 1) or drugs as indicated for 24 h. Western blotting was performed using 50 μg of cell lysates harvested after treatment and separated by SDS-PAGE.